

Transverse spin densities from lattice QCD

QCDSF and UKQCD Collaborations: M. Göckeler,^a Ph. Hägler*,^b R. Horsley,^c Y. Nakamura,^d D. Pleiter,^d P.E.L. Rakow,^e A. Schäfer,^a G. Schierholz,^{f,d} H. Stübgen^g and J.M. Zanotti^c

^a*Institut für Theoretische Physik, Universität Regensburg, 93040 Regensburg, Germany*

^b*Institut für Theoretische Physik T39, Physik-Department der TU München, James-Franck-Straße, 85747 Garching, Germany*

^c*School of Physics, University of Edinburgh, Edinburgh EH9 3JZ, UK*

^d*John von Neumann-Institut für Computing NIC / DESY, 15738 Zeuthen, Germany*

^e*Theoretical Physics Division, Department of Mathematical Sciences, University of Liverpool, Liverpool L69 3BX, UK*

^f*Deutsches Elektron-Synchrotron DESY, 22603 Hamburg, Germany*

^g*Konrad-Zuse-Zentrum für Informationstechnik Berlin, 14195 Berlin, Germany*

Email: phaegler@ph.tum.de

We present selected results from recent lattice QCD calculations of moments of quark helicity flip generalized parton distributions (GPDs) and transverse spin densities of quarks in the nucleon. Our dynamical simulations are based on two flavors of clover-improved Wilson fermions and Wilson glue. The large number of datasets for different values of β and κ allows us to study scaling violations and the pion mass dependence of our results. We find significant contributions from some of the quark helicity flip GPDs, giving rise to strongly distorted quark densities in impact parameter space.

*XXIVth International Symposium on Lattice Field Theory
July 23-28, 2006
Tucson, Arizona, USA*

*Speaker.

1. Introduction

This work is part of a systematic effort by the QCDSF/UKQCD collaboration to investigate the structure of hadrons (see e.g. [1–5]), and in particular the spin structure of the nucleon [6], in lattice QCD. Thanks to their probability density interpretation, generalized parton distributions (GPDs) in impact parameter space [7] are an extremely valuable tool for the study of the transverse spin structure of the nucleon [8]. Lattice results for transverse spin densities of quarks in the nucleon not only show distinct correlations of spin and coordinate degrees of freedom [4, 9], but they may also for the first time allow for predictions on intrinsic transverse momentum dependent distribution functions like the Sivers and the Boer-Mulders functions [10], which can be accessed experimentally in semi-inclusive DIS and Drell-Yan scattering [11–13]. Basic building blocks of the transverse spin density (to be defined in section 3) are the twist-2 quark helicity flip (tensor) GPDs H_T , \tilde{H}_T and \bar{E}_T [8, 14], which parametrize nucleon matrix elements of the bilocal tensor operator on the light-cone:

$$\begin{aligned} \langle P' \Lambda' | \int_{-\infty}^{\infty} \frac{d\eta}{4\pi} e^{i\eta x} \bar{q}\left(-\frac{\eta}{2}n\right) n_\mu \sigma^{\mu\nu\perp} \gamma_5 \mathcal{U} q\left(\frac{\eta}{2}n\right) | P \Lambda \rangle \\ = \bar{u}(P', \Lambda') n_\mu \left\{ \sigma^{\mu\nu\perp} \gamma_5 \left(H_T(x, \xi, t) - \frac{t}{2m^2} \tilde{H}_T(x, \xi, t) \right) + \frac{\varepsilon^{\mu\nu\perp\alpha\beta} \Delta_\alpha \gamma_\beta}{2m} \bar{E}_T(x, \xi, t) \right. \\ \left. - \frac{\Delta^{[\mu} \sigma^{\nu\perp]\alpha} \gamma_5 \Delta_\alpha}{2m^2} \tilde{H}_T(x, \xi, t) + \frac{\varepsilon^{\mu\nu\perp\alpha\beta} \bar{P}_\alpha \gamma_\beta}{m} \tilde{E}_T(x, \xi, t) \right\} u(P, \Lambda), \end{aligned} \quad (1.1)$$

where $\nu_\perp = 1, 2$, $f^{[\mu\nu]} = f^{\mu\nu} - f^{\nu\mu}$, $\Delta = P' - P$ is the momentum transfer with $t = \Delta^2$, $\bar{P} = (P' + P)/2$, and $\xi = -n \cdot \Delta/2$ defines the longitudinal momentum transfer with the light-like vector n . The Wilson line ensuring gauge invariance of the bilocal operator is denoted by \mathcal{U} .

In the forward limit, $\Delta = 0$, H_T is equal to the transversity distribution, $H_T(x, 0, 0) = \delta q(x) = h_1(x)$ for $x > 0$ and $H_T(x, 0, 0) = -\delta \bar{q}(-x) = -\bar{h}_1(-x)$ for $x < 0$. Furthermore, the integral of $H_T(x, \xi, t)$ over x gives the tensor form factor: $\int_{-1}^1 dx H_T(x, \xi, t) = g_T(t)$. Essential for our investigations is the probability density interpretation of the GPDs in impact parameter space for $\xi = 0$ [7]. For e.g. the quark GPD $H_q(x, \xi = 0, t)$ one finds that

$$q(x, b_\perp^2) \equiv \int \frac{d^2\Delta_\perp}{(2\pi)^2} e^{-ib_\perp \cdot \Delta_\perp} H_q(x, \xi = 0, t = -\Delta_\perp^2) \quad (1.2)$$

is the probability density for finding an unpolarized quark of flavor q with longitudinal momentum fraction x and position $b_\perp = (b_x, b_y)$ relative to the center of momentum in a nucleon.

For the computation of the tensor GPDs in lattice QCD, we transform the LHS of Eq. (1.1) to Mellin space by forming the integral $\int_{-1}^1 dx x^{n-1} \dots$, resulting in nucleon matrix elements of towers of local tensor operators

$$\mathcal{O}_T^{\mu\nu\mu_1\dots\mu_{n-1}}(0) = \mathcal{A}_{\mu\nu} \mathcal{S}_{\nu\mu_1\dots\mu_{n-1}} \bar{q}(0) \sigma^{\mu\nu} \gamma_5 i\overleftrightarrow{D}^{\mu_1} \dots i\overleftrightarrow{D}^{\mu_{n-1}} q(0) - \text{traces}, \quad (1.3)$$

which are parametrized in terms of tensor generalized form factors (GFFs) A_{Tni} , \bar{B}_{Tni} , \tilde{A}_{Tni} and \tilde{B}_{Tni} . Here, $\overleftrightarrow{D} = \frac{1}{2}(\overrightarrow{D} - \overleftarrow{D})$, and \mathcal{S} and \mathcal{A} denote symmetrization and anti-symmetrization respectively.

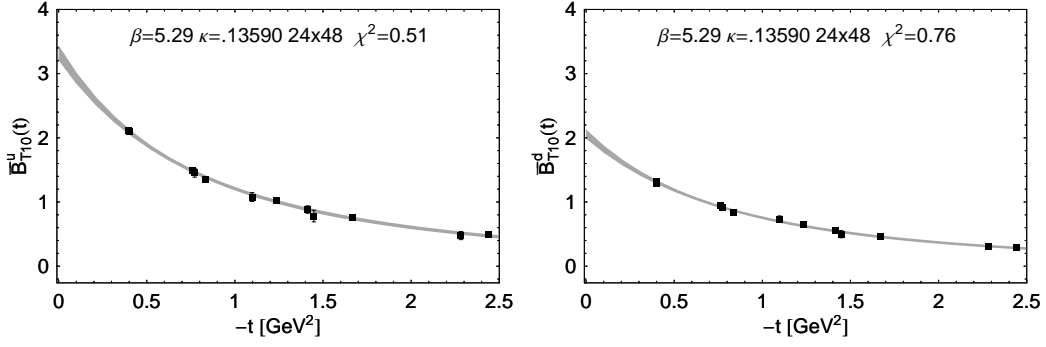


Figure 1: Results for the lowest moment of the GPD $\bar{E}_T(x, 0, t)$ for up (left) and down (right) quarks for a given β, κ -combination. Corresponding p-pole fits are shown by the shaded error bands.

For the lowest moment $n = 1$, we have [14, 16]

$$\begin{aligned} \langle P' \Lambda' | \mathcal{O}_T^{\mu\nu} | P \Lambda \rangle = & \bar{u}(P', \Lambda') \left\{ \sigma^{\mu\nu} \gamma_5 \left(A_{T10}(t) - \frac{t}{2m^2} \tilde{A}_{T10}(t) \right) \right. \\ & \left. + \frac{\varepsilon^{\mu\nu\alpha\beta} \Delta_\alpha \gamma_\beta}{2m} \bar{B}_{T10}(t) - \frac{\Delta^{[\mu} \sigma^{\nu]\alpha} \gamma_5 \Delta_\alpha}{2m^2} \tilde{A}_{T10}(t) \right\} u(P, \Lambda). \end{aligned} \quad (1.4)$$

The parametrization for higher moments $n \geq 1$ in terms of GFFs and their relations to the moments of the GPDs can be found in [16].

2. Numerical results for the lowest two moments of the tensor GPDs

The calculation of moments of GPDs in lattice QCD follows standard methods based on nucleon two- and three-point functions and has been described in detail in the literature [1, 3, 17].

This work is based on lattice simulations with $n_f = 2$ flavors of dynamical non-perturbatively $\mathcal{O}(a)$ improved Wilson fermions and Wilson glue. Computations have been performed at four different couplings $\beta = 5.20, 5.25, 5.29, 5.40$ with up to five different $\kappa = \kappa_{\text{sea}}$ values per β , corresponding to lattice spacings as small as 0.07 fm and pion masses as low as 400 MeV. The scale has been set using $r_0 = 0.467$ fm. The computationally demanding disconnected contributions are not included in this analysis. We expect, however, that they are small for the tensor GFFs [3]. We use non-perturbative renormalization [18] to transform our results to the $\overline{\text{MS}}$ scheme at a scale of 4 GeV². More details of the simulation can be found in [2, 3, 19].

In Fig. 1, we show results for the lowest moment of the GPD $\bar{E}_T(x, \xi, t)$ (called $\bar{B}_{T10}(t)$) as a function of the momentum transfer squared t . The lattice parameters in this case are $\beta = 5.29$, $\kappa = 0.13590$, corresponding to a pion mass of $m_\pi \approx 600$ MeV and a lattice spacing of $a \approx 0.08$ fm. For the extrapolation to the forward limit ($t = 0$) and in order to get a functional parametrization of the lattice data, we fit all our GFFs (generically denoted by $F(t)$) using a p-pole ansatz

$$F(t) = \frac{F(0)}{(1 - t/(pm_p^2))^p}, \quad (2.1)$$

depending on the three parameters $F(0)$, m_p and p . It turns out that in most cases we do not

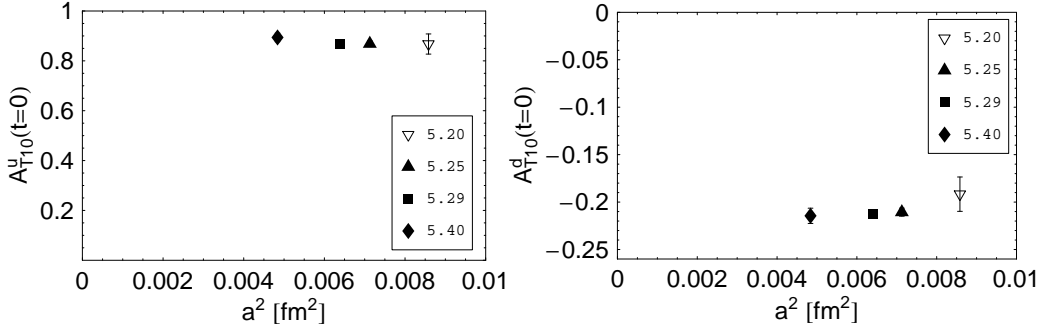


Figure 2: Study of discretization errors of the tensor charge $A_{T10}(0) = g_T(0)$ for up (LHS) and down (RHS) quarks at a pion mass of $m_\pi \approx 600$ MeV.

have sufficient statistics to determine all three parameters from a single fit to the data. For a given generalized form factor, we therefore fix the power p first by hand, guided by fits to selected datasets, where p is not allowed to vary with β and κ . The forward value $F(0)$ and the p-pole mass m_p are subsequently determined by a fit to the lattice data. For the examples in Fig. 1, we find $\bar{B}_{T10}^u(0) = 3.32(10)$ with $m_p = 0.882(87)$ GeV (for $p = 2.2$) and $\bar{B}_{T10}^d(0) = 2.06(6)$ with $m_p = 0.900(53)$ GeV (for $p = 2.5$). We have checked that the fits do not show a strong dependence on the exact value of p . In order to determine to what extent our calculation is affected by discretization errors, we plot as an example in Fig. 2 the tensor charge $A_{T10}(0) = g_T(0)$ versus the lattice spacing squared. The pion mass is approximately held fixed at $m_\pi \approx 600$ MeV. Within errors, the results do not show a clear dependence on a . At the same time, the still limited number of β values does not allow for a definite extrapolation to the continuum limit. We will therefore neglect any a dependence of the GFFs and leave a more careful study of the continuum limit for future works.

The pion mass dependence of the lowest moment of the GPD $\bar{E}_T(x, 0, t = 0)$ is shown in Fig. 3. Since we cannot expect the recent one-loop calculations in chiral perturbation theory [20] to be applicable to our data, we refrain from using them to extrapolate our results to the physical pion mass. Following common practice, we extrapolate the forward moments and the p-pole masses to the physical pion mass using a linear ansatz of the form $a + bm_\pi^2$. The results of the corresponding fits are shown as shaded error bands in Fig. 3. At $m_\pi = 140$ MeV, we find $\bar{B}_{T10}^u(0) = 3.13(19)$ and $\bar{B}_{T10}^d(0) = 1.94(12)$. These comparatively large values already indicate a significant contribution from this tensor GPD to the (transverse) spin structure of the nucleon, as will be discussed in the next section. Since the (tensor) GPD $\bar{E}_T(x, \xi, t)$ can be seen as the analogue of the (vector) GPD $E(x, \xi, t)$, we may define an anomalous tensor magnetic moment [10], $\kappa_T \equiv \int dx \bar{E}_T(x, \xi, 0) = \bar{B}_{T10}(0)$, similar to the standard anomalous magnetic moment $\kappa = \int dx E(x, \xi, 0) = B_{10}(0) = F_2(0)$. While the anomalous magnetic moments of the up and the down quark are both large and of opposite sign, $\kappa_{\text{exp}}^{\text{up}} \approx 1.67$ and $\kappa_{\text{exp}}^{\text{down}} \approx -2.03$, we find large positive values for the anomalous tensor magnetic moments for both flavors, $\kappa_{\text{T,latt}}^{\text{up}} \approx 3.13$ and $\kappa_{\text{T,latt}}^{\text{down}} \approx 1.94$.

3. Lattice results for the lowest two moments of the transverse spin density

The x^{n-1} -moment of the density of transversely polarized quarks (with spin vector s_\perp) in a

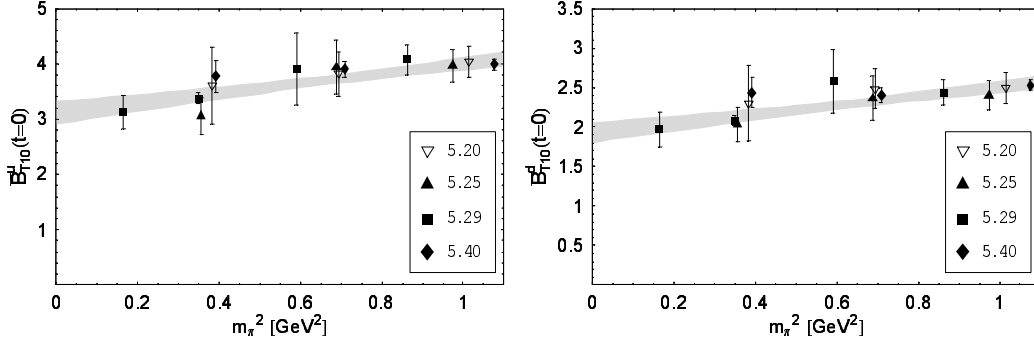


Figure 3: Pion mass dependence of the lowest moment of the GPD $\bar{E}_T(x, 0, t = 0)$ for up (left) and down (right) quarks. The shaded error band shows an extrapolation to the physical pion mass based on an ansatz linear in m_π^2 .

transversely polarized nucleon (with spin vector S_\perp) at impact parameter b_\perp is given by [8]

$$\rho^n(b_\perp) = \frac{1}{2} \int_{-1}^1 dx x^{n-1} \left(F + s_\perp^j F_T^j \right) = \frac{1}{2} \left\{ A_{n0}(b_\perp^2) + s_\perp^i S_\perp^i \left(A_{Tn0}(b_\perp^2) - \frac{1}{4m^2} \Delta_{b_\perp} \tilde{A}_{Tn0}(b_\perp^2) \right) + \frac{b_\perp^j \varepsilon^{ji}}{m} \left(S_\perp^i B'_{n0}(b_\perp^2) + s_\perp^i \bar{B}'_{Tn0}(b_\perp^2) \right) + s_\perp^i (2b_\perp^i b_\perp^j - b_\perp^2 \delta^{ij}) S_\perp^j \frac{1}{m^2} \tilde{A}''_{Tn0}(b_\perp^2) \right\}. \quad (3.1)$$

Definitions of the functions F and F_T^j can be found in Ref. [8]. The impact parameter dependent GFFs $A_{n0}(b_\perp^2)$, $A_{Tn0}(b_\perp^2)$, ... in Eq. (3.1) are related to the momentum space GFFs $A_{n0}(t)$, $A_{Tn0}(t)$, ... by a Fourier transformation as in Eq. (1.2). Their derivatives are defined by $f' \equiv \partial_{b_\perp^2} f$ and $\Delta_{b_\perp} f \equiv 4 \partial_{b_\perp^2} (b_\perp^2 \partial_{b_\perp^2}) f$.

For the numerical evaluation of Eq. (3.1), we Fourier transform the p-pole parametrization in Eq. (2.1) to impact parameter space and take all required derivatives with respect to b_\perp . The (derivatives of) GFFs in impact parameter space then depend only on the p-pole mass m_p and the forward value $F(0)$, both of which have been linearly extrapolated to the physical pion mass, and the power p .

Based on these results, we show in Fig. 4 the lowest moment of the spin density for a transversely polarized quark $s_\perp = (s_x, 0)$ in an unpolarized nucleon. The lowest moment of the density is strongly distorted in positive b_y direction for up and for down quarks due to the large positive values for the tensor GFFs $\bar{B}_{T10}^u(0)$ and $\bar{B}_{T10}^d(0)$ (see previous section). This is in strong contrast to the distortions one finds for unpolarized quarks in a transversely polarized nucleon [4, 9, 21], where the down quark density is distorted in negative b_y direction, due to the large and negative anomalous magnetic moment $\kappa_{\text{exp}}^{\text{down}} = B_{10}^d(0) \approx -2.03$.

It has been argued by Burkardt [10] that the shifted densities in Fig. 4 are related to a non-vanishing Boer-Mulders function [22] h_1^\perp which describes the correlation of intrinsic quark transverse momentum and the transverse quark spin s_\perp . According to [10] we have in particular $\kappa_T \sim -h_1^\perp$. Following this conjecture, the lattice results presented in this work for the first time strongly indicate that the Boer-Mulders function is large and negative both for up and down quarks. It would be highly interesting to confirm this in experiment, e.g. through measurement of azimuthal

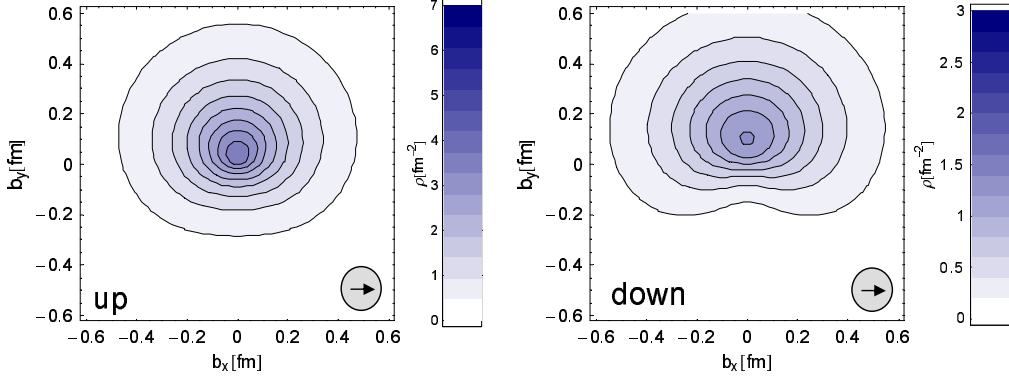


Figure 4: Lowest moment ($n = 1$) of the density of transversely polarized quarks in an unpolarized nucleon for up (left) and down (right) quarks. The quark spins are oriented in the transverse plane as indicated, where the inner arrow represents the quark spin vector s_{\perp} .

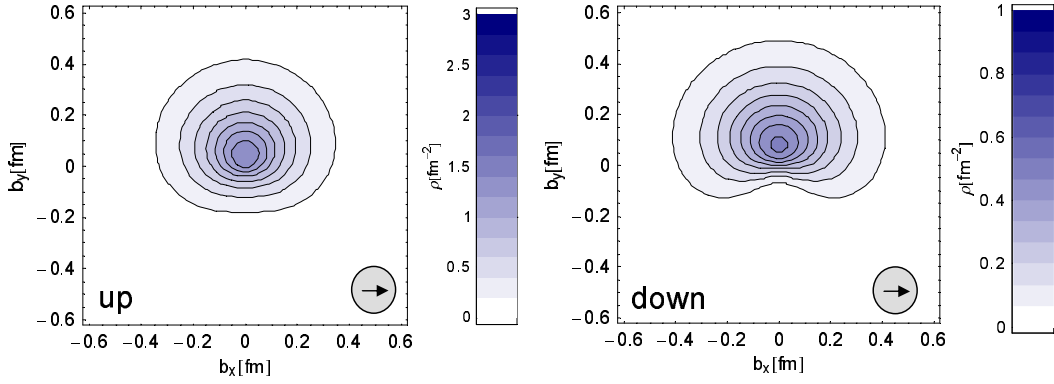


Figure 5: Second ($n = 2$) moment of the density of transversely polarized quarks in an unpolarized nucleon for up (left) and down (right) quarks. Symbols are explained in caption of Fig. 4

asymmetries in semi-inclusive meson production at JLab [12] and in unpolarized Drell-Yan scattering at GSI/PANDA [13].

An important question is whether the pattern we observe for the lowest moment of the density in Fig. 4 is generic and to what extent it changes for higher moments of the density. In a first attempt to address this question, we show in Fig. 5 the $n = 2$ -moment of the density. Encouragingly, the direction and magnitude of the distortion is very similar to the lowest moment in Fig. 4. The main difference is that the densities for the higher $n = 2$ -moment are more peaked around the origin $b_{\perp} = 0$. This is expected and confirms what has been observed in lattice calculations in [15] and [2].

4. Conclusions and outlook

We have presented first lattice results for moments of quark helicity flip GPDs for up and down quarks with pion masses as low as 400 MeV. Within errors, we do not observe a significant dependence of the extracted observables on the lattice spacing. We have extrapolated our results to the physical pion mass using an ansatz linear in m_{π}^2 . The lowest moments of the GPD \bar{E}_T turn out to be large and positive for up and for down quarks, giving rise to strongly distorted spin densities for transversely polarized quarks in an unpolarized nucleon. According to Burkardt [10], this leads

to the prediction of a sizeable negative Boer-Mulders function [22] for up and down quarks, which may be confirmed in experiments at e.g. JLab and GSI [12, 13].

Further results and details of our comprehensive lattice study of the helicity flip GPDs and transverse spin densities will be presented in a separate publication [23].

Acknowledgments

The numerical calculations have been performed on the Hitachi SR8000 at LRZ (Munich), the Cray T3E at EPCC (Edinburgh), the APE1000 and apeNEXT at NIC/DESY (Zeuthen) and the BlueGeneL at NIC/Jülich. This work was supported by the DFG (Forschergruppe Gitter-Hadronen-Phänomenologie and Emmy-Noether program) and by the EU I3HP under contract number RII3-CT-2004-506078.

References

- [1] M. Göckeler *et al.*, Phys. Rev. Lett. **92** (2004) 042002 [hep-ph/0304249].
- [2] M. Göckeler *et al.*, Nucl. Phys. A **755** (2005) 537 [hep-lat/0501029].
- [3] M. Göckeler *et al.*, Phys. Lett. B **627** (2005) 113 [hep-lat/0507001].
- [4] M. Göckeler *et al.*, Nucl. Phys. Proc. Suppl. **153** (2006) 146 [hep-lat/0512011].
- [5] D. Brömmel *et al.*, hep-lat/0608021; M. Göckeler *et al.*, hep-lat/0609001.
- [6] A. Ali Khan *et al.*, hep-lat/0603028.
- [7] M. Burkardt, Phys. Rev. D **62** (2000) 071503 [Erratum-ibid. D **66** (2002) 119903] [hep-ph/0005108].
- [8] M. Diehl and Ph. Hägler, Eur. Phys. J. C **44** (2005) 87 [hep-ph/0504175].
- [9] M. Diehl *et al.*, hep-ph/0511032.
- [10] M. Burkardt, Phys. Rev. D **72** (2005) 094020 [hep-ph/0505189].
- [11] A. Airapetian *et al.*, Phys. Rev. Lett. **94** (2005) 012002 [hep-ex/0408013].
- [12] H. Avakian *et al.*, JLab proposal PR12-06-112 (approved as first priority experiment).
- [13] M. Kotulla *et al.* [PANDA Collaboration], Letter of intent for PANDA.
- [14] M. Diehl, Eur. Phys. J. C **19** (2001) 485 [hep-ph/0101335].
- [15] Ph. Hägler *et al.*, Phys. Rev. Lett. **93** (2004) 112001 [hep-lat/0312014].
- [16] Ph. Hägler, Phys. Lett. B **594** (2004) 164 [hep-ph/0404138]; Z. Chen and X. Ji, Phys. Rev. D **71** (2005) 016003 [hep-ph/0404276].
- [17] Ph. Hägler *et al.*, Phys. Rev. D **68** (2003) 034505 [hep-lat/0304018].
- [18] G. Martinelli *et al.*, Nucl. Phys. B **445** (1995) 81 [hep-lat/9411010]; M. Göckeler *et al.*, Nucl. Phys. B **544** (1999) 699 [hep-lat/9807044].
- [19] M. Göckeler *et al.*, Few Body Syst. **36** (2005) 111 [hep-lat/0410023].
- [20] S. I. Ando, J. W. Chen and C. W. Kao, hep-ph/0602200; M. Diehl, A. Manashov and A. Schäfer, hep-ph/0608113.
- [21] M. Burkardt, Int. J. Mod. Phys. A **18** (2003) 173 [hep-ph/0207047].
- [22] D. Boer and P. J. Mulders, Phys. Rev. D **57** (1998) 5780 [hep-ph/9711485].
- [23] M. Göckeler *et al.*, *in preparation*.